

See discussions, stats, and author profiles for this publication at: <https://www.researchgate.net/publication/6651814>

Optimized expression vector for ion channel studies in *Xenopus* oocytes and mammalian cells using alfalfa mosaic virus

ARTICLE in PFLÜGERS ARCHIV - EUROPEAN JOURNAL OF PHYSIOLOGY · MAY 2007

Impact Factor: 4.1 · DOI: 10.1007/s00424-006-0183-1 · Source: PubMed

CITATIONS

24

READS

26

6 AUTHORS, INCLUDING:



Srinivasan Venkatachalan

9 PUBLICATIONS 168 CITATIONS

[SEE PROFILE](#)



Jeremy D Bushman

6 PUBLICATIONS 75 CITATIONS

[SEE PROFILE](#)



Jose L Mercado

University of Washington Seattle

9 PUBLICATIONS 151 CITATIONS

[SEE PROFILE](#)



Andrew Boileau

SABA University School of Medicine

14 PUBLICATIONS 597 CITATIONS

[SEE PROFILE](#)

Published in final edited form as:

Pflugers Arch. 2007 April ; 454(1): 155–163. doi:10.1007/s00424-006-0183-1.

Optimized expression vector for ion channel studies in *Xenopus* oocytes and mammalian cells using alfalfa mosaic virus

Srinivasan P. Venkatachalan¹, Jeremy D. Bushman¹, José L. Mercado², Feyza Sancar², Kelly R. Christopherson³, and Andrew J. Boileau¹

¹ Department of Physiology, University of Wisconsin-Madison, 601 Science Drive, Madison, WI 53711, USA e-mail: boileau@wisc.edu

² Neuroscience Training Program, University of Wisconsin-Madison, 601 Science Drive, Madison, WI 53711, USA

³ Molecular and Cellular Pharmacology Program, University of Wisconsin-Madison, 601 Science Drive, Madison, WI 53711, USA

Abstract

Plasmid vectors used for mammalian expression or for in vitro cRNA translation can differ substantially and are rarely cross-compatible. To make comparisons between mammalian and *Xenopus* oocyte expression systems, it would be advantageous to use a single vector without the need for shuttle vectors or subcloning. We have designed such a vector, designated pUNIV for *universal*, with elements that will allow for in vitro or ex vivo expression in multiple cell types. We tested the expression of pUNIV-based cDNA cassettes using enhanced green fluorescent protein and two forms of the type A γ -aminobutyric acid receptor (GABA_AR) and compared pUNIV to vectors optimized for expression in either *Xenopus* oocytes or mammalian cells. In HEK293 cells, radioligand binding was robust, and patch clamp experiments showed that subtle macroscopic GABA_AR kinetics were indistinguishable from our previous results. In *Xenopus* oocytes, agonist median effective concentration measurements matched previous work using a vector optimized for oocyte expression. Furthermore, we found that expression using pUNIV was significantly enhanced in oocytes and was remarkably long-lasting in both systems.

Keywords

Plasmid; Alfalfa mosaic virus (AMV); Episomal replication; tsA201/HEK293T cells; Beta-globin

Introduction

Proteins have been produced in a multitude of heterologous expression systems, including bacteria, yeast, plant tissue, and vertebrate cells [37]. The oocyte of *Xenopus laevis* has been a useful expression system for many proteins of interest [45], and a variety of mammalian cell lines are also available for *ex vivo* studies of protein function. In the neurosciences, laboratories studying ion channels often use these cells for characterization of conductances resulting from voltage steps, as with voltage-dependent ion channels or from application of agonists or drugs. We study a member of the ligand-gated ion channel superfamily (which includes acetylcholine, glycine, and serotonin receptor subtypes) the γ -aminobutyric acid receptor (GABA_AR). This

Correspondence to: Andrew J. Boileau.

Jeremy D. Bushman and José L. Mercado contributed equally to this work.

receptor is ubiquitous in the mammalian central nervous system and has homologues in other vertebrates and invertebrates [48]. It is composed of five subunits, from a diversity of subtypes, arranged pseudosymmetrically around a chloride-conducting pore. In the central nervous system, the most common stoichiometry for GABA_ARs is two α , two β , and one γ subunit [46]. However, α and β subunits can also assemble to form functional GABA_ARs without addition of the γ subunit [44,47].

Mutational studies of the GABA_AR have commonly been performed using *Xenopus* oocytes. Some mutations cause a severe reduction in GABA-gated currents, making high expression levels desirable. In addition, some studies require fast agonist application rates, such that the relatively large (~1-mm diameter) oocyte becomes impossible to superfuse rapidly enough to observe actual current rise times. For these studies, it behooves us to use smaller cells, such as transformed mammalian HEK293 cells. However, moving mutations of interest from one vector optimized for oocyte expression to a mammalian-specific expression vector requires additional effort of subcloning or redundant mutagenesis. Therefore, we designed and tested a single vector (pUNIV for *universal*) to yield high level, stable expression in multiple cell types.

The oocyte expression vector pGH19 (a derivative of pGEMHE: [31,39]) includes both 5'- and 3'-untranslated regions (UTRs) from the *Xenopus* β -globin gene [28] to stabilize injected cRNA and thereby boost expression several-fold [31,43]. It has been demonstrated that polyadenylation signals also stabilize cRNA transcripts in oocytes beyond 48 h [12], and slight changes in the 5'-UTR sequence can impact stability [43]. Along with the 3'-UTR from pGH19, pUNIV uses the alfalfa mosaic virus (AMV) coat protein (RNA 4) 5'-UTR. This AMV sequence has been shown to enhance in vitro translation [25] and expression of cRNA in oocyte studies [9,33], as well as in plant and bacterial expression systems [10,14,15]. We show that the combination of AMV plus β -globin stabilization boosts expression, compared to already high-level expression vectors for *Xenopus* oocytes and mammalian cells. Moreover, in both mammalian and oocyte expression systems, pUNIV expression levels remain elevated for days or even weeks.

Materials and methods

Plasmid construction

The backbone of pUNIV (Fig. 1) is the mammalian expression vector pCI-neo (Promega, Madison, WI), which contains a T7 promoter for in vitro cRNA transcription and a chimeric intron from human β -globin and an immunoglobulin gene heavy chain variable region [6,22,42] that may boost expression [8]. The large T-antigen acts on the SV40 origin of replication in pUNIV to allow for transient episomal replication [18,21,38], whereas pCEP4 (Invitrogen, Carlsbad, CA) uses Epstein-Barr viral sequences to promote episomal replication [36]. Both pUNIV and pCEP4 contain cytomegalovirus immediate early enhancer and promoter signals for mammalian expression [41]. cDNA for rat GABA_A α 1, β 2, γ 2S (short) and γ 2L (long splice variant) subunits were amplified using a 5' oligonucleotide containing an *Eco*R I site followed by the AMV sequence segment (GTTTTTATTTTAAATTTTCTTTCAAA TACTTCCACC) immediately before the start methionine of each subunit, and a 3' primer with an *Mlu* I site after the stop codon. This sequence was modified from the original, such that if the next base is an adenosine, an *Nco* I site is formed [25]. However, none of the clones presented here made use of this site, as we did not wish to alter the signal peptide sequence beyond the start methionine (though a version of pUNIV with AMV permanently inserted with an *Nco* I site could be constructed if desired). Therefore, the AMV was included by polymerase chain reaction (PCR) in the 5' oligonucleotide as opposed to being placed permanently in the vector. We inserted *Xenopus* β -globin polyadenylation sequence into the multiple cloning region of pCI-neo, PCR amplified from pGH19 with oligonucleotide primers (courtesy of Paul Gardner,

HHMI, University of Chicago) containing *Mlu* I (5') and *Not* I (3') restrictions sites. We also constructed pUNIV-EGFP with enhanced green fluorescent protein (Clontech, Mountain View, CA) as an independent marker for transfection efficiency.

Mammalian cell culture

Cells were grown on 100-or 35-mm tissue culture dishes in minimum essential medium with Earle's salts (Life Technologies) containing 10% fetal bovine serum (Hyclone Laboratories) in a 37°C incubator under a 5% CO₂ atmosphere. HEK293 cells were from the American Type Culture Collection (CRL 1573), HEK293T cells were kindly provided by Dr. Robert Macdonald (Vanderbilt University), and tsA201 cells were kindly provided by Dr. J. Michael Edwardson (University of Cambridge). HEK293T and tsA201 are derived from the same line of HEK293 cells (*293tsA1609neo*) stably transfected with the temperature sensitive gene for SV40 T-antigen [13]. We will refer to this line as tsA201 henceforth to distinguish from our standard HEK293 cells.

Radioligand binding assays

For radioligand binding assays, cells were cotransfected at 25–50% confluency with cDNA for α 1, β 2, and γ 2L subunits in either pCEP4 or pUNIV using a standard CaHPO₄ method [19]. For [³H]muscimol binding estimates of apparent affinity, we transfected cells with 4 μ g/subunit in pCEP or pUNIV. For [³H]flunitrazepam (FNZM) estimations of maximal binding, 6 μ g/subunit in pCEP or 3 μ g/subunit in pUNIV were used to maintain similar copy number. Cells were incubated at 31°C/4% CO₂ before harvesting.

Cells were harvested approximately 48 h after transfection, membrane homogenates were prepared, and homologous competition binding experiments were performed as described previously [2,40]. In brief, membrane homogenates (100 μ g) were incubated at room temperature for 1 h with sub-K_d concentrations of radioligand ([³H]muscimol, 28.1 Ci/mmol or [³H]FNZM, 84.5 Ci/mmol; NEN Life Sciences, Boston, MA) in the absence or presence of up to seven different concentrations of corresponding unlabeled ligand (ranging from 0.3 nM to 10 μ M) in a final volume of 250 μ l. Specific binding was defined as [³H]drug bound in the absence of displacing ligand minus the amount bound in the presence of displacing ligand (10 μ M). Data were fit by nonlinear regression to a one-site competition curve defined by the equation $y = B_{\max}/[1 + (x/IC_{50})]$, where y is bound [³H]ligand in dpm, B_{\max} is maximal binding, x is the concentration of displacing ligand, and IC_{50} is the concentration of unlabeled ligand that inhibits 50% of [³H]ligand binding (GraphPad Prism; GraphPad Software, San Diego, CA). Because radioactive and nonradioactive ligands were chemically identical, K_I values were calculated using a simplified Cheng–Prusoff/Chou equation: $K_I = IC_{50} - [L^*]$, where K_I refers to the equilibrium dissociation constant of the radioligand and $[L^*]$ refers to the concentration of radioactive ligand used.

B_{\max} values for FNZM were determined as described previously [40]. Specific binding of [³H]FNZM to membrane homogenates was measured using a sub-K_d concentration of [³H]FNZM in triplicate. The B_{\max} values were then calculated using $B = [(B_{\max} \times [L])/([L] + K_I)]$, where B is the measured specific [³H]FNZM binding in dpm, $[L]$ is the concentration of [³H]FNZM used in the experiment and K_I is the apparent binding affinity of FNZM (10 nM), averaged from multiple competition binding assays from our laboratory [2,29,30,40]. Nonradioactive FNZM was obtained as a gift from Dr. Sepinwall (Hoffman-La Roche, Nutley, NJ), and nonradioactive muscimol was from Sigma.

Mammalian cell recording

Whole cell recording from tsA201 cells was performed as described previously for HEK293 cells [5]. Cells were plated in 35-mm culture dishes 24–72 h before transient transfection with

pCEP or pUNIV cDNAs for rat $\alpha 1$, $\beta 2$, and $\gamma 2L$ subunits. We used 200 ng of $\alpha 1$ and $\beta 2$ to express $\alpha\beta$ receptors and added 2,000 ng $\gamma 2L$ for $\alpha\beta\gamma$ receptors cotransfected with 100–200 ng pCEP-EGFP or pUNIV-EGFP for visualization of transfected cells using a mercury lamp. Cells were transfected at 70–90% confluency using 3 μ l Lipofectamine2000 (Invitrogen). Cells were refed 4–8 h after transfection, passaged to new 35-mm plates, and replated on 12-mm circular cover glass (Fisher Scientific, Pittsburgh, PA) 1 to 4 h before experiments, and maintained at 31°C to prevent overgrowth.

Solutions were applied using a two-barrel theta application pipette (Warner Instruments, Holliston, MA) connected to a piezoelectric stacked translator (Physik Instrumente, Costa Mesa, CA). The rapid application system was constructed of Teflon and polyimide tubing (Cole-Parmer, Vernon Hills, IL) connected to the theta glass. The voltage input to the high voltage amplifier (Physik Instrumente) used to drive the stacked translator was filtered (90 Hz) using an 8-pole Bessel Filter (Frequency Devices, Haverhill, MA) to reduce oscillations arising from rapid acceleration of the pipette. After obtaining stable whole cell access, negative holding pressure was applied, and the cell was lifted from the coverslip and positioned in front of the application pipette.

The recording chamber was perfused continuously with 4-2-hydroxyethyl-1-piperazineethanesulfonic acid (HEPES)-buffered saline containing (mM): 145 NaCl, 5 KCl, 1 MgCl₂, 1.8 CaCl₂, 10 HEPES; pH 7.4. This standard saline was also used as the “control” solution in the rapid application pipette. Recording pipettes were filled with: (mM) KCl 130, ethylene glycol bis(2-aminoethyl ether)-*N,N,N',N'*-tetraacetic acid 5, HEPES 10, MgCl₂ 1, MgATP (ATP, adenosine triphosphate) 5; pH 7.2. GABA solutions were prepared daily from powder and diluted to desired concentrations in the same control/bath solution. Recordings were performed at room temperature on the stage of a Nikon TE-2000-S microscope.

Recording electrodes were fabricated from KG-33 glass (Garner Glass Company, Claremont, CA) using a multistage puller (Flaming–Brown model P-87, Sutter Instruments, Novato, CA) and coated with Sylgard 184 (Dow Corning, Midland, MI) to reduce electrode capacitance. The tips were fire polished. Open tip electrode resistance was typically 1–4 M Ω when filled with standard recording solution. All recordings were obtained at a holding potential of –40 mV unless otherwise specified using an Axopatch 200B amplifier (Axon Instruments, Foster City, CA). Access resistance, typically 2–3 M Ω , was compensated >80% using amplifier circuitry. Data were low-pass filtered at 2–5 kHz, sampled at 5–10 kHz, and stored online using pClamp 9 software (Axon Instruments).

Oocyte expression and voltage-clamp

Mature stage V–VI oocytes from *Xenopus laevis* were defolliculated using 1 mg/ml collagenase Type 1A (Sigma, St. Louis, MO). cRNA was transcribed from *Not* I-linearized pUNIV or *Nhe* I-linearized pGH19 using the T7 mMessage mMachine kit (Ambion, Austin, TX). Defolliculated oocytes were injected with 27.4 nl of cRNA at a concentration of 50 pg/nl per subunit of $\alpha 1$ and $\beta 2$ subunits for $\alpha\beta$ receptors or 5:5:50 pg/nl ($\alpha 1/\beta 2/\gamma 2$) to produce $\alpha 1\beta 2\gamma 2$ receptors [4]. Oocytes were incubated at 18°C in ND96 (in mM: 96 NaCl, 2 KCl, 1 MgCl₂, 1.8 CaCl₂, and 5 HEPES, pH 7.2) supplemented with 100 μ g/ml gentamycin and 100 μ g/ml bovine serum albumin for 2–14 days before use. GABA (Sigma) solutions were prepared daily in ND96.

Oocytes were continuously perfused at a rate of 5 ml/min with ND96 in a 1.5 mm wide \times 1.5-mm deep trough in Plexiglas with a metal post to hold the oocyte in place under flow. Oocytes were held under two-electrode voltage clamp at –80 mV. Borosilicate electrodes (Warner Instruments, Hamden, CT) were filled with 3 M KCl and had resistances between 0.7 to 2 M Ω . Electrophysiological data were acquired with a GeneClamp 500 (Axon Instruments)

interfaced to a computer with an ITC16 analog-to-digital device (Instrutech, Great Neck, NY) and recorded using Whole Cell Program 3.2.9 (kindly provided by J. Domspter; University of Strathclyde, Glasgow, Scotland).

Concentration-response experiments were performed as described previously [3,32]. In brief, GABA concentration-responses were scaled to a low, nondesensitizing concentration of GABA (EC_2 – EC_{10}) applied just before the test concentration to correct for any slow drift in I_{GABA} over the course of the experiment. Currents elicited by each test concentration were normalized to the corresponding low concentration current before curve fitting. Concentration-response data were fit to the following equation: $I = I_{max}/(1 + (EC_{50}/[A])^n)$, where I is the peak response to a given concentration of GABA; I_{max} is the maximum amplitude of current; median effective concentration (EC_{50}) is the concentration of GABA that evokes half-maximal response; $[A]$ is the agonist concentration; and n is the Hill coefficient (Graphpad Prism).

Statistics

Comparisons between two data sets used either an unpaired t -test (nonparametric, Mann–Whitney test) or a paired t -test with a nonparametric correction (Wilcoxon matched pair test) when appropriate (Graphpad Prism). For comparisons of multiple data sets, one-way analysis of variance was employed, with Dunnett's or Bonferroni post-tests for significance of difference.

Results

Vector construction

The universal vector pUNIV was constructed using pCI-neo as backbone (Fig. 1; see Materials and methods). The *Xenopus* β -globin 3'-UTR and polyA tail was inserted to improve cRNA stability [28] and boost expression in oocytes [31,43]. A modified AMV sequence was engineered into the 5' PCR primer for each insert (in this case, EGFP or GABA_AR subunit cDNAs) and incorporated in place of any native Kozak sequences [27]. pUNIV constructs were then linearized with *Not* I for cRNA transcription and injection into *Xenopus* oocytes or transfected whole into HEK293 or tsA201 cells.

Mammalian cell experiments

We first confirmed expression of GABA_ARs composed of $\alpha 1$ and $\beta 2$ subunits using a radioligand binding assay and compared pUNIV expression directly to our standard vector, pCEP4 [1,5]. We measured the apparent affinity (K_d) for muscimol, an agonist at the GABA binding site, by homologous competition of [³H]muscimol with cold muscimol (Fig. 2a). No significant difference was found between pCEP4 and pUNIV in three comparisons (all in HEK293 cells), with a pooled K_d of 67.4 ± 12.2 nM, similar to values previously obtained [40].

We also tested the ability of the large T-antigen stably expressed in tsA201 cells to enhance expression of subunit cDNAs in pUNIV by assaying benzodiazepine binding to $\alpha 1\beta 2\gamma 2L$ receptors. Benzodiazepines require a γ subunit for their activity at the GABA_AR [34] and bind to fully assembled pentameric receptors, whereas muscimol can bind to $\alpha\beta$ receptors or partially assembled receptors [23]. We found dramatically increased [³H]FNZM binding of pUNIV-transfected tsA201 cells compared to pCEP4-transfected HEK293 cells (Fig. 2b), indicating a higher maximal number of binding sites expressed. B_{max} with pUNIV was significantly higher (3.4-fold, $p=0.007$) than with pCEP4 in paired determinations ($n=4$).

Before performing electrophysiological recordings, we optimized transfection efficiency using EGFP-containing constructs. In multiple experiments, we found significantly lower expression

of pUNIV-EGFP in our standard HEK293 cell line compared to pCEP4 (data not shown). Conversely, pCEP4-EGFP expression in tsA201 cells was less than optimal. However, pairing pUNIV constructs with tsA201 cells gave robust expression. GABA-gated currents from pUNIV GABA_AR constructs were indistinguishable from previous recordings with pCEP4 constructs in HEK293 cells and were robust for at least 7 days (Fig. 3a). We further confirmed that macroscopic desensitization (Fig. 3b) and deactivation kinetics (Fig. 3c) were not altered from the use of AMV.

Expression in *Xenopus* oocytes

Having established that pUNIV would provide long-term expression in mammalian cells, we next compared pUNIV to the high-level expression vector for oocyte studies, pGH19. Currents expressed in oocytes were qualitatively similar for pUNIV and pGH19 (Fig. 4a).

Concentration-response profiles (Fig. 4b) showed no significant differences ($p > 0.05$) for the receptors expressed from either vector. EC₅₀ values and Hill coefficients were as follows (mean \pm s.d., $n \geq 4$): pUNIV $\alpha 1\beta 2$ EC₅₀ 1.6 ± 0.3 μ M, Hill 1.3 ± 0.2 ; pGH19 $\alpha 1\beta 2$ EC₅₀ 2.1 ± 0.3 μ M, Hill 1.2 ± 0.2 ; pUNIV $\alpha 1\beta 2\gamma 2$ EC₅₀ 15 ± 2 μ M, Hill 1.5 ± 0.1 ; pGH19 $\alpha 1\beta 2\gamma 2$ EC₅₀ 13 ± 1 μ M, Hill 1.5 ± 0.2 .

In a 2-week time-course, we found that pUNIV cRNA was at least as long lasting as pGH19 for both $\alpha 1\beta 2$ (Fig. 4c) and $\alpha 1\beta 2\gamma 2$ S receptors (data not shown). However, the pUNIV expression was significantly higher throughout the course of the experiment, with the exception of the first day postinjection (Fig. 4c). Maximal currents for $\alpha 1\beta 2$ receptors from pGH19 constructs were 10.3 ± 1.1 μ A (mean \pm s.e.m.) on day 5 postinjection, whereas pUNIV constructs yielded 14.7 ± 1.0 μ A. By day 13, average currents from pGH19 constructs were 7.5 ± 1.1 μ A versus 13.0 ± 0.9 μ A for pUNIV constructs. Similar results, with pUNIV constructs outstripping pGH19 constructs, were obtained for $\alpha 1\beta 2\gamma 2$ S receptors (data not shown).

Discussion

We have engineered a general use vector for both mammalian and oocyte expression systems. This allows for more direct comparison of proteins of interest or mutations from one system to the other without time-intensive subcloning or the need for shuttle vectors. Furthermore, any vector-dependent changes in protein expression, modification, or posttranslational behavior should be eliminated. Compared to two available vectors already optimized for high-expression in mammalian cells (pCEP4) or *Xenopus laevis* oocyte expression (pGH19), the new vector pUNIV performed as well or better. Expression was long lasting, exceeding 1 week, and quite robust. Receptors were also shown to behave similarly to previous work, using more sensitive kinetic comparisons (Fig. 3).

The long-term stability of cRNAs in oocytes from both pUNIV and pGH19 may be due to the addition of the *Xenopus* β -globin 3'-UTR and polyA signal. We speculate that the increased expression in oocytes using the pUNIV vector (Fig. 4c) was due to the inclusion of the AMV sequence before the start methionine. It is possible that the AMV sequence also accounts for much of the increase in expression seen in HEK293 cell lines (Fig. 2b). The unstructured nature of the AMV RNA 4 leader sequence may allow for more competitive expression compared to native mRNAs, because it does not require unwinding or association with cap-binding proteins [16,35], or it may have increased affinity for other (perhaps limiting) components of the translation machinery [25]. For example, efficient in vitro translation using AMV has a reduced requirement for elongation factors [7]. Other vectors have employed "optimized" Kozak sequences for enhancing expression [11,17]; we found that replacing any of our native Kozak sequences with AMV in pUNIV worked more efficiently.

We excluded any GFP coexpression element in pUNIV unlike other vectors [24], as this may interfere with fluorescence studies and has also been suggested to produce cytotoxic effects [20,26]. For identification of transfected HEK293 cells for electrophysiology experiments, we used EGFP coexpression at controlled, lower levels. However, other identification methods could easily have been used, such as antitag antibody bead-labeling. For bacterial expression using the T7 promoter, any of a variety of protein purification tags can be incorporated into the 5' oligonucleotide, such as a maltose-binding protein tag to increase protein solubility [11].

Concluding remarks

High-level expression is particularly useful when studying ion channels with low amplitude or mutations that reduce expression levels, and long-lasting expression is necessary when multiple recordings over a time-course would be required (e.g. after reinjection with an additional cRNA). By boosting expression, pUNIV will also provide an advantage when expressing proteins on a larger preparative scale. On the other end of the spectrum, higher expression levels require less of any limiting reagent, and increased signal-to-noise ratios will be beneficial for studies, such as radioligand binding assays or labeled fluorescence experiments. Ability to study a protein across expression systems is not only timesaving but may alert us to differences that are system-dependent.

Acknowledgements

We thank Dr. Cynthia Czajkowski for support and encouragement and Mark Nowak for helpful discussions. This work was funded by National Institute of Health grants MH66406 to C.C./A.B. and NS34727 to C.C.

References

1. Boileau AJ, Pearce RA, Czajkowski C. Tandem subunits effectively constrain GABA_A receptor stoichiometry and recapitulate receptor kinetics but are insensitive to GABA_A receptor-associated protein. *J Neurosci* 2005;25:11219–11230. [PubMed: 16339017]
2. Boileau AJ, Kucken AM, Evers AR, Czajkowski C. Molecular dissection of benzodiazepine binding and allosteric coupling using chimeric γ -aminobutyric acid_A receptor subunits. *Mol Pharmacol* 1998;53:295–303. [PubMed: 9463488]
3. Boileau AJ, Evers AR, Davis AF, Czajkowski C. Mapping the agonist binding site of the GABA_A receptor: evidence for a β -strand. *J Neurosci* 1999;19:4847–4854. [PubMed: 10366619]
4. Boileau AJ, Baur R, Sharkey LM, Sigel E, Czajkowski C. The relative amount of cRNA coding for γ 2 subunits affects stimulation by benzodiazepines in GABA_A receptors expressed in *Xenopus* oocytes. *Neuropharmacology* 2002;43:695–700. [PubMed: 12367615]
5. Boileau AJ, Li T, Benkwitz C, Czajkowski C, Pearce RA. Effects of γ 2S subunit incorporation on GABA_A receptor macroscopic kinetics. *Neuropharmacology* 2003;44:1003–1012. [PubMed: 12763093]
6. Bothwell AL, Paskind M, Reth M, Imanishi-Kari T, Rajewsky K, Baltimore D. Heavy chain variable region contribution to the NPb family of antibodies: somatic mutation evident in a gamma 2a variable region. *Cell* 1981;24:625–637. [PubMed: 6788376]
7. Browning KS, Lax SR, Humphreys J, Ravel JM, Jobling SA, Gehrke L. Evidence that the 5'-untranslated leader of mRNA affects the requirement for wheat germ initiation factors 4A, 4F, and 4G. *J Biol Chem* 1988;263:9630–9634. [PubMed: 3260235]
8. Buchman AR, Berg P. Comparison of intron-dependent and intron-independent gene expression. *Mol Cell Biol* 1988;8:4395–4405. [PubMed: 3185553]
9. Dahan DS, Dibas MI, Petersson EJ, Auyeung VC, Chanda B, Bezanilla F, Dougherty DA, Lester HA. A fluorophore attached to nicotinic acetylcholine receptor beta M2 detects productive binding of agonist to the alpha delta site. *Proc Natl Acad Sci USA* 2004;101:10195–10200. [PubMed: 15218096]

10. Dai Z, Hooker BS, Quesenberry RD, Thomas SR. Optimization of *Acidothermus cellulolyticus* endoglucanase (E1) production in transgenic tobacco plants by transcriptional, post-transcription and post-translational modification. *Transgenic Res* 2005;14:627–643. [PubMed: 16245154]
11. Donnelly MI, Zhou M, Millard CS, Clancy S, Stols L, Eschenfeldt WH, Collart FR, Joachimiak A. An expression vector tailored for large-scale, high-throughput purification of recombinant proteins. *Protein Expr Purif* 2006;47:446–454. [PubMed: 16497515]
12. Drummond DR, Armstrong J, Colman A. The effect of capping and polyadenylation on the stability, movement and translation of synthetic messenger RNAs in *Xenopus* oocytes. *Nucleic Acids Res* 1985;13:7375–7394. [PubMed: 3932972]
13. DuBridge RB, Tang P, Hsia HC, Leong PM, Miller JH, Calos MP. Analysis of mutation in human cells by using an Epstein–Barr virus shuttle system. *Mol Cell Biol* 1987;7:379–387. [PubMed: 3031469]
14. Fletcher L, Corbin SD, Browning KS, Ravel JM. The absence of a m7G cap on beta-globin mRNA and alfalfa mosaic virus RNA 4 increases the amounts of initiation factor 4F required for translation. *J Biol Chem* 1990;265:19582–19587. [PubMed: 2246243]
15. Gallie DR, Sleat DE, Watts JW, Turner PC, Wilson TM. A comparison of eukaryotic viral 5'-leader sequences as enhancers of mRNA expression in vivo. *Nucleic Acids Res* 1987;15:8693–8711. [PubMed: 2825117]
16. Gehrke L, Auron PE, Quigley GJ, Rich A, Sonenberg N. 5'-Conformation of capped alfalfa mosaic virus ribonucleic acid 4 may reflect its independence of the cap structure or of cap-binding protein for efficient translation. *Biochemistry* 1983;22:5157–5164. [PubMed: 6317016]
17. Georgiev O, Bourquin JP, Gstaiger M, Knoepfel L, Schaffner W, Hovens C. Two versatile eukaryotic vectors permitting epitope tagging, radiolabelling and nuclear localisation of expressed proteins. *Gene* 1996;168:165–167. [PubMed: 8654937]
18. Gluzman Y. SV40-transformed simian cells support the replication of early SV40 mutants. *Cell* 1981;23:175–182. [PubMed: 6260373]
19. Graham FL, van der Eb AJ. Transformation of rat cells by DNA of human adenovirus 5. *Virology* 1973;54:536–539. [PubMed: 4737663]
20. Hanazono Y, Yu JM, Dunbar CE, Emmons RV. Green fluorescent protein retroviral vectors: low titer and high recombination frequency suggest a selective disadvantage. *Hum Gene Ther* 1997;8:1313–1319. [PubMed: 9295126]
21. Heinzel SS, Krysan PJ, Calos MP, DuBridge RB. Use of simian virus 40 replication to amplify Epstein–Barr virus shuttle vectors in human cells. *J Virol* 1988;62:3738–3746. [PubMed: 2843671]
22. Huang MT, Gorman CM. The simian virus 40 small-t intron, present in many common expression vectors, leads to aberrant splicing. *Mol Cell Biol* 1990;10:1805–1810. [PubMed: 1690852]
23. Im WB, Pregenzer JF, Binder JA, Dillon GH, Alberts GL. Chloride channel expression with the tandem construct of $\alpha 6$ - $\beta 2$ GABA_A receptor subunit requires a monomeric subunit of $\alpha 6$ or $\gamma 2$. *J Biol Chem* 1995;270:26063–26066. [PubMed: 7592805]
24. Jespersen T, Grunnet M, Angelo K, Klaerke DA, Olesen SP. Dual-function vector for protein expression in both mammalian cells and *Xenopus laevis* oocytes. *Biotechniques* 2002;32:536–538. 540. [PubMed: 11911656]
25. Jobling SA, Gehrke L. Enhanced translation of chimaeric messenger RNAs containing a plant viral untranslated leader sequence. *Nature* 1987;325:622–625. [PubMed: 3492677]
26. Klein RL, Dayton RD, Leidenheimer NJ, Jansen K, Golde TE, Zweig RM. Efficient neuronal gene transfer with AAV8 leads to neurotoxic levels of tau or green fluorescent proteins. *Mol Ther* 2006;13:517–527. [PubMed: 16325474]
27. Kozak M. At least six nucleotides preceding the AUG initiator codon enhance translation in mammalian cells. *J Mol Biol* 1987;196:947–950. [PubMed: 3681984]
28. Krieg PA, Melton DA. Functional messenger RNAs are produced by SP6 in vitro transcription of cloned cDNAs. *Nucleic Acids Res* 1984;12:7057–7070. [PubMed: 6207484]
29. Kucken AM, Teissere JA, Seffinga-Clark J, Wagner DA, Czajkowski C. Structural requirements for imidazobenzodiazepine binding to GABA_A receptors. *Mol Pharmacol* 2003;63:289–296. [PubMed: 12527800]

30. Kucken AM, Wagner DA, Ward PR, Teiss re JA, Boileau AJ, Czajkowski C. Identification of benzodiazepine binding site residues in the $\gamma 2$ subunit of the γ -aminobutyric acid_A receptor. *Mol Pharmacol* 2000;57:932–939. [PubMed: 10779376]
31. Liman ER, Tytgat J, Hess P. Subunit stoichiometry of a mammalian K⁺ channel determined by construction of multimeric cDNAs. *Neuron* 1992;9:861–871. [PubMed: 1419000]
32. Mercado J, Czajkowski C. Charged residues in the $\alpha 1$ and $\beta 2$ pre-M1 regions involved in GABA_A receptor activation. *J Neurosci* 2006;26:2031–2040. [PubMed: 16481436]
33. Nowak MW, Kearney PC, Sampson JR, Saks ME, Labarca CG, Silverman SK, Zhong W, Thorson J, Abelson JN, Davidson N, et al. Nicotinic receptor binding site probed with unnatural amino acid incorporation in intact cells. *Science* 1995;268:439–442. [PubMed: 7716551]
34. Pritchett DB, Sontheimer H, Shivers BD, Ymer S, Kettenmann H, Schofield PR, Seeburg PH. Importance of a novel GABA_A receptor subunit for benzodiazepine pharmacology. *Nature* 1989;338:582–585. [PubMed: 2538761]
35. Ray BK, Lawson TG, Kramer JC, Cladaras MH, Grifo JA, Abramson RD, Merrick WC, Thach RE. ATP-dependent unwinding of messenger RNA structure by eukaryotic initiation factors. *J Biol Chem* 1985;260:7651–7658. [PubMed: 3838990]
36. Reisman D, Sugden B. trans activation of an Epstein–Barr viral transcriptional enhancer by the Epstein–Barr viral nuclear antigen 1. *Mol Cell Biol* 1986;6:3838–3846. [PubMed: 3025615]
37. Reyes-Ruiz JM, Barrera-Saldana HA. Proteins in a DNA world: expression systems for their study. *Rev Invest Clin* 2006;58:47–55. [PubMed: 16789599]
38. Rio DC, Clark SG, Tjian R. A mammalian host-vector system that regulates expression and amplification of transfected genes by temperature induction. *Science* 1985;227:23–28. [PubMed: 2981116]
39. Robertson GA, Warmke JM, Ganetzký B. Potassium currents expressed from *Drosophila* and mouse egg cDNAs in *Xenopus* oocytes. *Neuropharmacology* 1996;35:841–850. [PubMed: 8938715]
40. Sancar F, Czajkowski C. A GABA_A receptor mutation linked to human epilepsy ($\gamma 2$ R43Q) impairs cell surface expression of $\alpha\beta\gamma$ receptors. *J Biol Chem* 2004;279:47034–47039. [PubMed: 15342642]
41. Schmidt EV, Christoph G, Zeller R, Leder P. The cytomegalovirus enhancer: a pan-active control element in transgenic mice. *Mol Cell Biol* 1990;10:4406–4411. [PubMed: 2164640]
42. Senapathy P, Shapiro MB, Harris NL. Splice junctions, branch point sites, and exons: sequence statistics, identification, and applications to genome project. *Methods Enzymol* 1990;183:252–278. [PubMed: 2314278]
43. Shih TM, Smith RD, Toro L, Goldin AL. High-level expression and detection of ion channels in *Xenopus* oocytes. *Methods Enzymol* 1998;293:529–556. [PubMed: 9711627]
44. Sigel E, Baur R, Trube G, Mohler H, Malherbe P. The effect of subunit composition of rat brain GABA_A receptors on channel function. *Neuron* 1990;5:703–711. [PubMed: 1699569]
45. Stuhmer W. Electrophysiological recording from *Xenopus* oocytes. *Methods Enzymol* 1992;207:319–339. [PubMed: 1382188]
46. Tretter V, Ehya N, Fuchs K, Sieghart W. Stoichiometry and assembly of a recombinant GABA_A receptor subtype. *J Neurosci* 1997;17:2728–2737. [PubMed: 9092594]
47. Verdoorn TA, Draguhn A, Ymer S, Seeburg PH, Sakmann B. Functional properties of recombinant rat GABA_A receptors depend upon subunit composition. *Neuron* 1990;4:919–928. [PubMed: 1694446]
48. Xue H. Identification of major phylogenetic branches of inhibitory ligand-gated channel receptors. *J Mol Evol* 1998;47:323–333. [PubMed: 9732459]

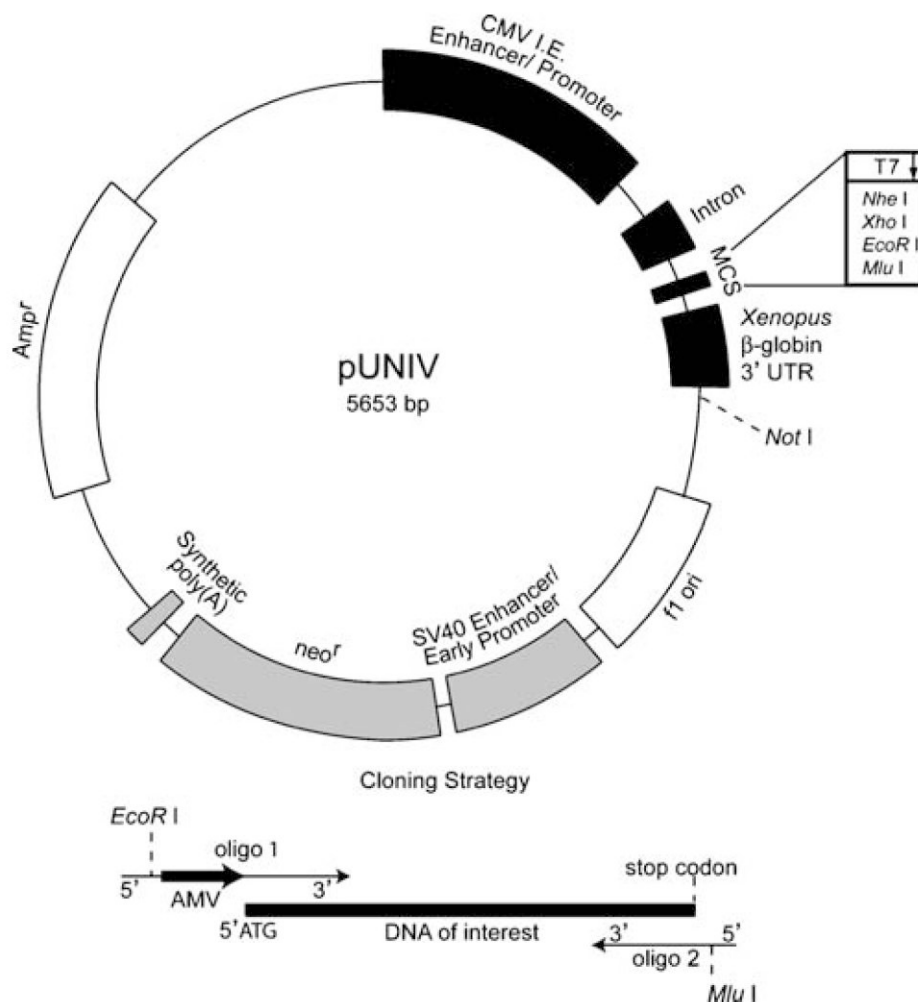
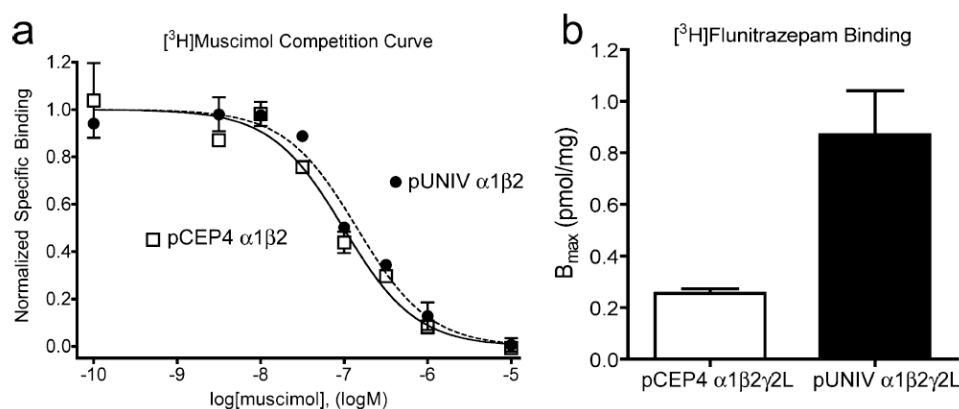
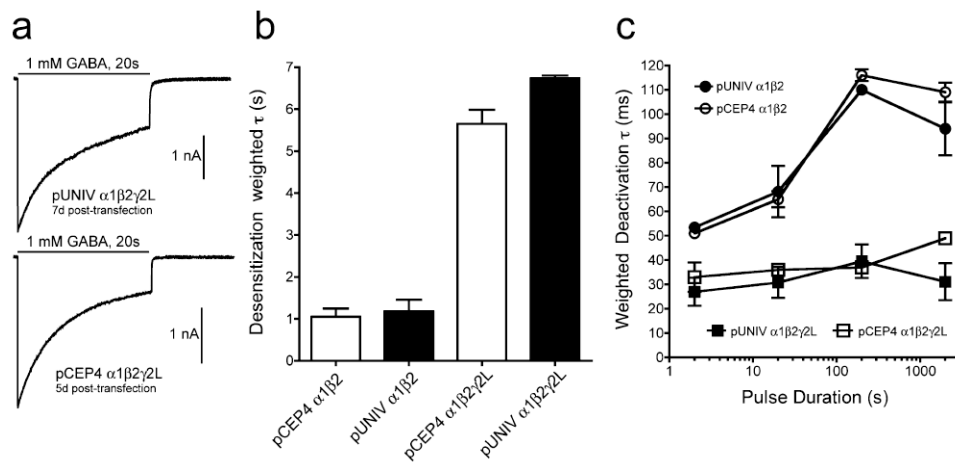


Fig. 1. pUNIV Construction. pUNIV was derived from the backbone vector pCI-neo, which contains an f1 origin of replication (*f1 ori*) and an ampicillin resistance gene (*Amp^r*) for maintenance in ampicillin-sensitive bacterial strains (*white segments*). pCI-neo also contains a neomycin phosphotransferase gene (*neo^r*) for G418 selection under the control of SV40 enhancer/promoter with an SV40 tail region downstream. This region (*gray*) also promotes episomal replication when coexpressed with the SV40 large T antigen or when expressed in a T antigen stable cell line. Expression features are *highlighted in black*. Mammalian expression is driven by the CMV immediate early enhancer/promoter, and cRNA transcription uses T7 RNA polymerase. The chimeric intron between the CMV promoter and the multiple cloning site (*MCS*) is also depicted (see Materials and methods). The inserted *Xenopus* β-globin 3'-UTR contains the polyadenylation signal. DNA of interest is PCR amplified with oligonucleotides designed to add restriction sites for directional subcloning into the MCS. The 5' oligonucleotide also contains the AMV sequence immediately prior to the start methionine (5' ATG) in the DNA of interest

**Fig. 2.**

Expression of GABA_ARs in HEK293 cells using pUNIV constructs. **a** Radioligand binding experiment with HEK293 cells transfected with pUNIV- $\alpha 1$ plus pUNIV- $\beta 2$ constructs (*closed circles*) versus pCEP4- $\alpha 1$ plus pCEP4- $\beta 2$ (*open squares*). Membrane homogenates were bound with $[^3\text{H}]\text{muscimol}$, a GABA agonist, and displaced with nonradioactive muscimol at varying concentrations (see Materials and methods). No significant difference was found between the two vector types. Data are mean \pm s.e.m., $n=3$. **b** Binding with $[^3\text{H}]\text{FNZM}$ to assess maximal binding (B_{max}) for pentameric receptors. Homogenates from transfections with pUNIV $\alpha 1\beta 2\gamma 2\text{L}$ in tsA201 cells (*closed bars*) were compared to pCEP4 $\alpha 1\beta 2\gamma 2\text{L}$ in HEK293 cells (*open bars*). pUNIV expression in a T-antigen-containing cell line was 3.4-fold higher in four paired comparisons ($p=0.007$). Data are mean \pm s.e.m

**Fig. 3.**

Electrophysiological recording of GABA_AR currents from pUNIV versus pCEP4 constructs. **a** Current traces comparing $\alpha 1\beta 2\gamma 2L$ receptors formed using pUNIV (top) or pCEP4 expression vectors (bottom) pulsed with maximal (10 mM) GABA for 20 s. Cells are 7 and 5 days posttransfection, respectively. Portions of these data are reprinted with permission [1]; Copyright 2005 by the Society for Neuroscience. **b** Weighted desensitization time constants (τ) for $\alpha 1\beta 2$ and $\alpha 1\beta 2\gamma 2L$ using either pUNIV (black bars) or pCEP4 (open bars) do not differ significantly between vectors ($\alpha 1\beta 2$, $p=1.0$; $\alpha 1\beta 2\gamma 2L$, $p=0.057$). Data are mean \pm s.e.m., $n \geq 3$. **c** Weighted deactivation time constants (τ) for $\alpha 1\beta 2$ and $\alpha 1\beta 2\gamma 2L$ transfections using the two expression vectors. pUNIV $\alpha 1\beta 2$ (closed circles) and pCEP4 $\alpha 1\beta 2$ (open circles) deactivation do not differ significantly ($p > 0.05$) at any pulse duration tested nor do pUNIV $\alpha 1\beta 2\gamma 2L$ (closed squares) compared to pCEP4 $\alpha 1\beta 2\gamma 2L$ (open squares). Data are mean \pm s.e.m., $n=3-12$. In some cases, error bars are smaller than symbols.

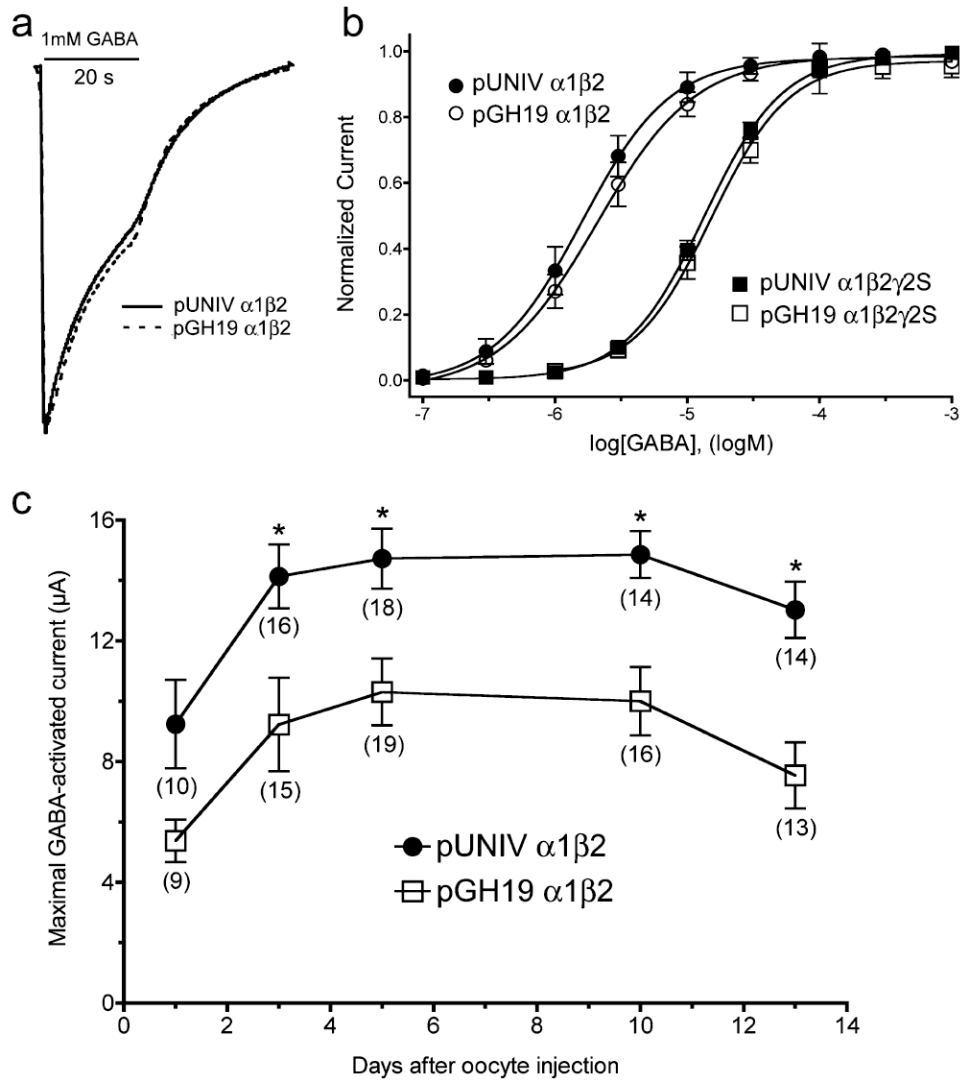


Fig. 4.

Expression of GABA_ARs in *Xenopus* oocytes is long-lasting and robust. **a** Typical current traces from oocytes injected with cRNA from pUNIV- $\alpha 1$ plus pUNIV- $\beta 2$ (solid trace) normalized and compared to pGH19- $\alpha 1$ plus pGH19- $\beta 2$ (dashed trace). Cells were exposed to 1 mM GABA for 20 s then washed back into recording solution. **b** Concentration-response curves for $\alpha 1\beta 2$ (circles) versus $\alpha 1\beta 2\gamma 2S$ GABA_ARs (squares) expressed from pUNIV (open symbols) or pGH19 (closed symbols). Peak currents at varying GABA concentrations were normalized to 10 mM GABA and fit with a sigmoidal concentration-response equation (see Materials and methods). EC₅₀ values and Hill slopes for either receptor type were not significantly different between the two vectors. Data are mean \pm s.e.m., $n \geq 3$. **c** Time-course for expression levels of $\alpha 1\beta 2$ receptors. Peak currents with 10 mM GABA were measured for cells injected with cRNA from pUNIV (closed circles) versus pGH19 (open squares) over a 2-week time period. pUNIV currents were statistically larger than pGH19 currents for days 3, 5, 10, and 13 postinjection (asterisk). p values were as follows: day 1, $p=0.079$; day 3, $p=0.014$; day 5, $p=0.0037$; day 10, $p=0.0034$; day 13, $p=0.0021$. Data are mean \pm s.e.m. Number of experiments per time point (n) in parentheses